

Chapter IX. Numerical modelling of interaction between gravity waves and elastic ice floes (*I.V. Lavrenov, A.V. Novakov*)

Self-consistent movement of liquid and elastic fluctuations of ice plates particularly covering the liquid is simulated numerically in a linear statement of a problem. A task is to solve the Laplace's equation for liquid and the equation of elastic fluctuations of ice floe both. The numerical and analytical solutions, which are defined by integral equation with Green function, are compared. To solve the problem numerically a method of boundary elements for Laplace's equation and to solve equation for elastic ice plate a method of finite elements are proposed to use. The coefficients of passage and reflection of surface gravity waves by floating plates were obtained. A conclusion was made that the solution can be the quasi-periodic one. It is defined by the initial parameters of waves and ice plates. Ice floes can make filter influence on the surface wave spectrum decreasing significantly some components, which are composed to the most reflection.

Swell waves can penetrate into the zones of broken up and compact ice from the open sea. A lot of experimental data for waves with ice were obtained by MIZEX experiment (1). Observations of waves penetrating under the compacted ice are described in publication (2). Particularly, it is pointed out that long waves under the ice cover can penetrate at significant distances and have high amplitudes and even break up the compacted ice (3).

The methods to simulate the interaction between gravitation waves and concentrated ice cover or semi-infinite ice plate were well tackled (4, 5). An attempt to simulate waves in shallow water areas with floating ice floes of finite length was made in publication (6) in order to estimate the wave spectrum evolution with presence of ice. Ice was simulated by absolutely stiff floating ice floes. However, according to calculation results, the interaction between gravitation wave and elastic ice plate differs from that between the inelastic one.

There are many difficulties to solve the problem of interaction between gravity waves and ice floe of finite length. The task is to solve both the Laplace's equation for liquid and equation of thin elastic plate bending, which includes the fourth spatial derivative.

In approximation of shallow water the solution of a problem was presented in publication (7), where it was pointed out that bandwidths of gravitation waves can appear even with presence of infinite sequence of floating ice floes of finite length.

The problems of diffraction of bending-gravitation waves in ice with cracks and fractures were described in publications (8, 9). Analytical solution of a problem for deep water by deducing to integral equation using a method of Green's function was obtained in publication (10). But such method allows to solve a problem only for specific ideal conditions (infinite deep bottom, uniformity of parameters of ice plate along its entire length etc.).

To overcome such limits the numerical solution of a problem is proposed in this article. Numerical implementation was performed on the base of modern method of finite and boundary elements. Therewith, a statement of a problem close to that in publication (10) was used. It allowed to compare the calculation results with analytical solution. In this article more common problem is solved. Particularly, the reflectivity and penetration of waves not only from one or two, but from also from a system of three and four ice floes with different length is calculated. An effect of internal stressful condition is accounted.

1. Statement of a problem. The uniform isotropic ice plate with length L is floating on surface of ideal liquid (Fig. 1). The origin of coordinates is on free liquid surface and Z-axis is directed vertically down. The linearized boundary task for speed potential $\phi(x, z, t)$ for incompressible and unrotating liquid is the following:

$$\left. \begin{aligned} \nabla^2 \phi &= 0; & 0 < z < H \\ \frac{\partial \phi}{\partial z} &= 0; & z = H \\ \frac{\partial \phi}{\partial z} &= -\frac{\partial \zeta}{\partial t}; & -\rho \left(g \frac{\partial \phi}{\partial z} - \frac{\partial^2 \phi}{\partial t^2} \right) = -\frac{\partial p}{\partial t}; & z = 0 \end{aligned} \right| \quad (1)$$

where g — free fall acceleration, p — pressure on the liquid surface, ρ — water density, ζ — deviation of free surface, H — depth of liquid.

If a plate is uniform and isotropic, its displacement from equilibrium position is defined by biharmonic oscillation equation:

$$\left. \frac{\partial^2 \zeta}{\partial t^2} + \mu^2 \frac{\partial^4 \zeta}{\partial x^4} = \frac{p}{\rho' h}; \quad z = 0; \quad 0 < x < L \right|$$

So, a boundary condition under ice plate is written in the following way:

$$\left. -\rho \left(g \frac{\partial \phi}{\partial z} - \frac{\partial^2 \phi}{\partial t^2} \right) = \rho' h \left(\frac{\partial^3 \phi}{\partial^2 t \partial z} + \mu^2 \frac{\partial^5 \phi}{\partial^4 x \partial z} \right); \quad z = 0; 0 < x < L \right| \quad (2)$$

Let suppose that for the open water the expression is the following $\partial p / \partial t = 0$:

$$\left. g \frac{\partial \phi}{\partial z} - \frac{\partial^2 \phi}{\partial t^2} = 0; \quad z = 0; \quad -\infty < x < 0; \quad L < x < \infty \right| \quad (3)$$

For the ice edge the conditions of free edge are to be true, i.e. bending moment and intersecting force are equal to zero [11]:

$$\left. \frac{\partial^2 \zeta}{\partial x^2} = \frac{\partial^3 \zeta}{\partial x^3} = 0; \quad x = 0; \quad x = L; \quad z = 0 \right| \quad (4)$$

In equations (2)—(4) the following notations are used: ρ' is ice density, $\mu^2 = Eh^2 / 12\rho'(1 - \nu^2)$, E — Young module, h — ice floe thickness, ν — Poisson coefficient.

Considering the solution to be periodical in time, let define the solution as $\phi = \phi' e^{i\omega t}$ for infinitely deep liquid. Therefore, the problem can be rewritten in the following way (there are no dashes below):

$$\left. \begin{aligned} \nabla^2 \phi &= 0; & \infty < z < 0 \\ \frac{\partial \phi}{\partial z} &= 0; & z \rightarrow \infty \\ \frac{\partial \phi}{\partial z} + \frac{\omega^2}{g} \phi &= 0; & z = 0; \quad -\infty < x < 0; \quad L < x < \infty \\ \frac{\partial^5 \phi}{\partial x^4 \partial z} + \alpha^4 \frac{\partial \phi}{\partial z} + \beta \phi &= 0; & z = 0; \quad 0 < x < L \\ \frac{\partial^3 \phi}{\partial x^2 \partial z} = \frac{\partial^4 \phi}{\partial x^3 \partial z} &= 0; & x = 0; \quad x = L; \quad z = 0 \\ \alpha^4 &= -\frac{\omega^2}{\mu^2} + \frac{\rho g}{\rho' h \mu^2}; & \beta &= \frac{\omega^2 \rho}{\rho' h \mu^2} \end{aligned} \right| \quad (5)$$

Considering that a potential of coming wave has unit amplitude, the boundary condition with $x \rightarrow \pm\infty$ can be written in the following way:

$$\begin{aligned}\phi &= T \exp(-ikx - kz) && \text{при} && x \rightarrow \infty ; \\ \phi &= \exp(-ikx - kz) + R \exp(ikx - kz) && \text{при} && x \rightarrow -\infty .\end{aligned}$$

(6)

where: R and T — coefficients of reflection and travelling of wave accordingly.

An analytic solution of the problem (5), (6) as an integral equation of Fredholm is proposed in [10]:

$$R = ik \int_0^L e^{-ik\xi} \left[\phi(\xi, 0) + \beta \int_0^L \delta(\xi, \iota) \phi(\iota, 0) d\iota \right] d\xi \quad (1.7)$$

$$T = 1 + ik \int_0^L e^{ik\xi} \left[\phi(\xi, 0) + \beta \int_0^L \delta(\xi, \iota) \phi(\iota, 0) d\iota \right] d\xi \quad (1.8)$$

$$\phi(x, 0) = e^{-ikx} + k \int_0^L \left[G(\xi, 0; \zeta, 0) + i \cos(kr) \right] \left[\phi(\xi, 0) + \beta \int_0^L \delta(\xi, \iota) \phi(\iota, 0) d\iota \right] d\xi \quad (1.9)$$

where: G — Green's function in Laplace's equation, δ — Green's function in equation for elastic plate (2).

2. Numerical solution. To implement the problem numerically the methods of both boundary (for Laplace's equation approximation) and finite (for approximation of elastic plate equation) elements are used.

Accounting the Green's function characteristic

$$\frac{\partial \phi(x, 0)}{\partial z} = -\beta \int_0^L g(x, \xi) \phi(\xi, 0) d\xi \quad (10)$$

the equation for speed potential (6) is rewritten as

$$\phi(x, 0) = e^{-ikx} + \int_0^L \left[G(\xi, 0; \zeta, 0) + i \cos(kr) \right] \left[k\phi(\xi, 0) + \frac{\partial \phi(\xi, 0)}{\partial z} \right] d\xi \quad (11)$$

This equation was considered as boundary-element statement of a problem [12].

It is assumed that Green's function G in this expression should comply with boundary conditions on free surface and lower boundary. The following expression for G is proposed in [10]:

$$\begin{aligned}G(\xi, \zeta; x, z) &= \frac{1}{4\pi} \ln \left[(\xi - x)^2 + (\zeta - z)^2 \right] - \frac{1}{4\pi} \ln \left[(\xi - x)^2 + (\zeta + z)^2 \right] - \\ &- \frac{1}{2\pi} \int_{-\infty}^{\infty} \frac{1}{|\omega| - k} e^{-|\omega|(\zeta+z)} e^{i\omega(\xi-x)} d\omega\end{aligned}$$

On the surface ($z=\zeta=0$) this expression is deduced to

$$G(\xi, 0; x, 0) = -\frac{1}{\pi} \left(Ci(kr) \cos(kr) + \sin(kr) \left(Si(kr) + \frac{\pi}{2} \right) \right)$$

After performing the spatial quantization the expression (7) can be written in the following matrix form:

$$M_{ij}\phi_i + N_{ij} \frac{\partial \phi_i}{\partial z} = B_i \quad (12)$$

In this equation the matrix forms M и N depend on the selection of numerical integrating formulas.

Finite-element form of equation for ice plate taking (2) is written in the following way:

$$\int_{S(x)} \left[W_i \frac{\partial^5 \hat{\phi}}{\partial x^4 \partial z} + \alpha W_i \frac{\partial \hat{\phi}}{\partial z} \right] dS(x) - \beta \int_{S(x)} W_i \hat{\phi} dS = 0,$$

$$\alpha = \frac{\omega^2}{\mu^2} - \frac{\rho g}{\rho' h \mu^2}$$

$$\hat{\phi}(x) = \varphi_1(x)\phi_1 + \varphi_2(x)\phi_2 + \dots$$

where: $\varphi_i(x)$ — base functions, W_i — weight functions, which were assumed to be equal to the base ones according to the method of Bubnov-Galerkin.

Integrating the first integral twice by parts, in the left part we will define:

$$\int_{S(x)} \left[\frac{\partial^2 W_i}{\partial x^2} \frac{\partial^2 \varphi_j}{\partial x^2} + \alpha W_i \varphi_j \right] \frac{\partial \phi_i}{\partial z} dS(x) - \beta \int_{S(x)} W_i \varphi_j \phi_i dS(x) +$$

$$\left[W_i \frac{\partial^4 \hat{\phi}}{\partial x^3 \partial z} - \frac{\partial W_i}{\partial x} \frac{\partial^3 \hat{\phi}}{\partial x^2 \partial z} \right]^{x=0,L} = 0 \quad (13)$$

Accounting the boundary conditions on the ice plate edges (4), the last component in the left part of this expression is excluded:

Therefore, the equation (13) in a matrix type will be rewritten as

$$M'_{ij}\phi_i + N'_{ij} \frac{\partial \phi_i}{\partial z} = 0 \quad (14)$$

$$M'_{ij} = \int_{S(x)} \left[\frac{\partial^2 W_i}{\partial x^2} \frac{\partial^2 \varphi_j}{\partial x^2} + \alpha W_i \varphi_j \right] dS(x), \quad N'_{ij} = \beta \int_{S(x)} W_i \varphi_j dS(x)$$

It is necessary that not only the condition of the potential continuity on boundaries of elements should be fulfilled but the condition of continuity by x of its first derivative (13) as well selecting the finite elements.

So, to solve the boundary problem for Laplace's equation (1)—(5) it is necessary to solve two systems (12) and (14). Testing the numerical algorithm the numerical results and analytic solution were compared. Therewith, the difference between the obtained results and the analytical ones, which were defined solving the system (7), was not more than 10^{-6} .

3. Results of numerical modeling of interaction between waves and ice floe. In calculations presented in this section the physical parameters were used as follows: Young's module $E = 6 \cdot 10^9$ Pa, Poisson's coefficient for ice $\nu = 0,3$, densities of sea water and ice - 1025 kg/m^3 и $922,5$ kg/m^3 accordingly.

Proportions between the module of wave reflection coefficient $|R|$ and length of ice plate L for different wave lengths (10 m, 50 m and 200 m) are presented on Fig. 2. Each curve has

similar structure and is the sequence of curved up segments, in zero points of which $|R|=0$, i.e. wave travels under the ice plate without reflection with these parameters. Let name such zero points as the resonance ones according to terminology [10].

If $L/\lambda \gg 1$, the distance between the resonance points approximates to 1/2 of wave length under ice. If the length of ice plate is small, curve structure is not kept up. It can be explained by the influence of boundary effects with penetrating of wave under ice cover. Calculations show that these effects become evident when the ice plate length is less than $c_1\lambda'$ (λ' is wave length under ice, $c_1=0,80-0,85$ is the empiric coefficient). According to the calculations, the reflection coefficient module reaches the maximum value when the proportion between length of wave and ice plate is the following: $L \approx c_2\lambda_2$ ($c_2=0,55-0,60$).

Speed potential under ice plate (for $z=0$) is presented on Fig. 3 as a function of dimensionless coordinate x/L . Ice plate length is approximately equal to 366 m. It is one of the resonance lengths. Speed potential amplitude in marginal area is more than that in the middle of ice plate by 10-12 %. This value can change depending on proportion between lengths of wave and ice plate and reach 20 % in unresonance case. Actual potential part reaches the maximum value on the ice plate boundary, the imaginary one becomes equal to zero. It testifies that the horizontal speed of wave movements of liquid on the boundary (for $z=0$) becomes equal to zero, the wave phase changes to the contrary one.

Wave length under ice plate $\lambda=2\pi/k$ can be defined by a dispersion proportion. To obtain this proportion, let substitute the solution $\phi(x, z)=\exp(-ikx-kz)$ to the initial equations (5):

$$\omega^2 = \frac{gk + \frac{Eh^3k^5}{12\rho(1-\nu^2)}}{1 + \frac{\rho'hk}{\rho}} \quad (15)$$

Figure 4 presents a diagram, which demonstrates the proportion between wave length under ice cover λ' and ice thickness calculated by formula (15) for wave lengths $\lambda=50$ m, 100 m and 200 m on open water. So, waves penetrating under ice cover are longer than the initial ones on open water, therewith, they are transformed to the shorter waves.

When ice becomes thicker, the reflection coefficient increases. Accounting that ice thickness is a component of the dispersion equation (15), wave will be longer under the thicker ice. So, the distance between resonance points will be longer as well.

To solve the problem of interaction between waves and ice accounting the internal stress of ice cover the equation for ice plate will be the following:

$$\rho'h\mu^2 \frac{\partial^5\phi}{\partial x^4\partial z} + hP \frac{\partial^3\phi}{\partial x^2\partial z} + (\rho'h\omega^2 - \rho g) \frac{\partial\phi}{\partial z} - \omega^2\rho\phi = 0 \quad (16)$$

where P — internal stress in ice cover.

Presence of internal stress in ice cover brings to decrease of reflection of gravitation wave from the plate. Module of reflection coefficient increases with internal extension (Fig. 5).

Wave length under ice also depends on internal stress in ice. Calculated wave lengths λ' for ice extension $P = -10^6$ n/m² and ice pressure $P=10^6$ n/m² will accordingly be equal to 138,2 m and 114,2 m. So, the distance between resonance points will increase with internal extension and decrease with internal pressure.

Module of reflection coefficient depends on wave length not only qualitatively but quantitatively as well. The most evidently it is observed on an example of transformation of wave frequency spectrum due to the influence of floating ice floe. If wave length is 10 m length, the reflection coefficient becomes almost equal to 1. If wave length is 200 m it does not exceed 0.06. A conclusion can be made that reflection from ice plate becomes nonsignificant with very long waves. So, the high-frequency component of wave spectrum will be reflected by ice floe more intensely. However, the presence of resonance points can bring to that a part of spectrum range will penetrate under ice plate almost without obstacles. Figure 6 (a) represents changing of Pirson-Moskovits spectrum [14] after wave travelling under ice plate of 110 m length. The second maximum was formed at 0.45 Hz frequency in spectrum. The third maximum at 0.45 Hz can be revealed considering a more detailed diagram of high-frequency spectrum range (Fig. 6 (b)). 0.45 Hz frequency corresponds to wave length of about 7 m, i.e. even such short waves in some cases can penetrate under ice almost without reflection.

4. Results of numerical simulation of waves with some ice floes. The described method of solving the problem of interaction between gravitation waves and ice plate can be generalized for the case of some ice plates with ice edge coordinates: x_j, L_j (j is a number of ice plate):

$$\phi(x,0) = e^{-ikx} + \sum_j \int_{x_j}^{L_j} \left[G(\xi,0; \zeta,0) + i \cos(kr) \right] \left[k\phi(\xi,0) + \frac{\partial \phi(\xi,0)}{\partial z} \right] d\xi \quad (17)$$

Figure 7 presents the calculation results for cases of two, three and four ice plates. An aspect is of interest that a system consisting of some ice plates of finite length on certain conditions can have zero reflection, even in a case when each of these ice plates is not absolutely transparent for wave. However, such situation was observed only for ice plates of the same lengths. If ice plate lengths are selected arbitrarily, the reflection coefficient of a system did not reach zero. Figure 7 (a) presents the proportions between the reflection coefficient of the system consisting of two ice plates and the distance between ice plates. The proportion can transform to practically direct line with specific parameters (for example, for ice plates of 100 m and 175 m lengths).

General structure of curves is also sectional, and the distance between resonance points in this case corresponds to a half of wave length in open water. For the system consisting of three and four ice plates this period is kept. However, the additional maximums appear (one - for three ice plates, (Figure 7 (b)), two- for four ice plates (Figure 7, c) between the main maximums. The maximum of reflection coefficient increases when the number of ice plates increases as well.

Conclusion

There is such combination of system parameters when reflection does not occur (resonance points) during the propagation of gravitation wave under ice plate.

The reflection coefficient significantly depends on wave length and can change in a range from almost complete reflection up to some per cents with wave length of 200 m and longer. The reflection coefficient is maximum when ice plate length is $L \approx c_2 \lambda'$ ($c_2=0,55-0,60$).

When ice thickness increases, maximum reflection coefficient and distance between resonance points increase too.

If there is the internal stress in ice cover, the reflection coefficient and distance between resonance points decrease, for the case of internal extension they increase.

Reflectivity of a system consisting of some ice plates is less than that of any ice plate and can reach zero for a system consisting of ice plates of equal length. Period of a proportion between reflection coefficient module and distance between the ice plates is equal to a half of wave length on open water.

There is the filter influence of ice floes on surface wave spectrum: high-frequency component of wave spectrum reflects by ice floe more significantly than the low-frequency one. But, the local spectrum maximums can appear (also in its high-frequency range) because of the presence of resonance points.

This article was prepared in framework of an agreement on research cooperation between NPI and AARI Roshydromet (NP project 1707/201).

References

1. Wadhams P., V.A.Squire, J.A.Ewing & R.W. Paskal The effect of the marginal ice zone on the directional wave spectrum of the ocean// J. Phys. Oceanogr., 1986, V.16, №2, pp. 358-376
2. Squire V.A. How waves break up inshore fast ice// J. Polar Record., 1984, V.22, №138, Sept., pp. 281-285
3. Liu A.K. & E. Mollo-Christensen Wave propagation in a solid ice pack// J. Phys. Oceanogr., 1988, V.18, №11, pp. 1702-1712
4. Bukatov A.E., L.V. Cherkesov & A.A. Yaroshenko Bending-gravitation waves from moving perturbations// PMTF, 1984, №2, pp. 151-157
5. Fox C. & V.A. Squire Strain in shore fast ice due to incoming ocean waves and swell// J. Geophys. Res., 1991, V.96, №C3, pp. 4531-4547
6. Masson D. P.H. LeBlond Spectral evolution of wind-generated surface gravity waves in a dispersed ice field// J. Fluid Mech., 1989, V.202, pp. 43-81
7. Marchenko A., P. Purini & K. Voliak Filtering surface waves by the ice floes// Proc. 13th Intern. Conf. on Port and Ocean Eng. under Arctic Cond. (POAC'95. Murmansk). St.Petersburg, 1995, V.3, pp. 134-142
8. Marchenko A.V. Diffraction of bending-gravitation waves on linear heterogeneity in ice cover. Izv. RAN, MJG, 1997, №4, pp. 97-112
9. Marchenko A.& K. Voliak Surface wave propagation in shallow water beneath an inhomogeneous ice cover// J. Phys. Oceanogr., 1997, V.27, №8, pp. 1602-1613
10. Meylan M.& V.A. Squire The response of ice floes to ocean waves// J.Geophys. Res., 1994, V.99, №C1, pp. 891-900
11. Krasil'nikov V.N. Influence of thin resilient layer on the propagation of sound in liquid semi-space. Acoustics journal, 1960, V.6, Iss. 2, pp. 220-228
12. Brebbiya K., J. Telles & L. Vrowbel Methods of boundary elements. Moscow, Mir, 1987, p. 524
13. S'yarle F. Method of finite elements for elliptic problems. Moscow, Mir, 1980, p. 512
14. Davidan I.N., L.I. Lopatukhin & V.A. Rozhkov Wind waves in the World ocean. Leningrad, Gidrometeoizdat, 1985, p. 256

Figures

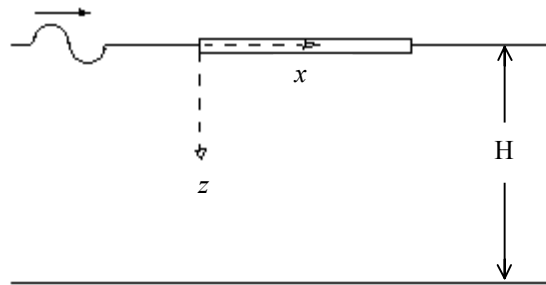


Figure 1

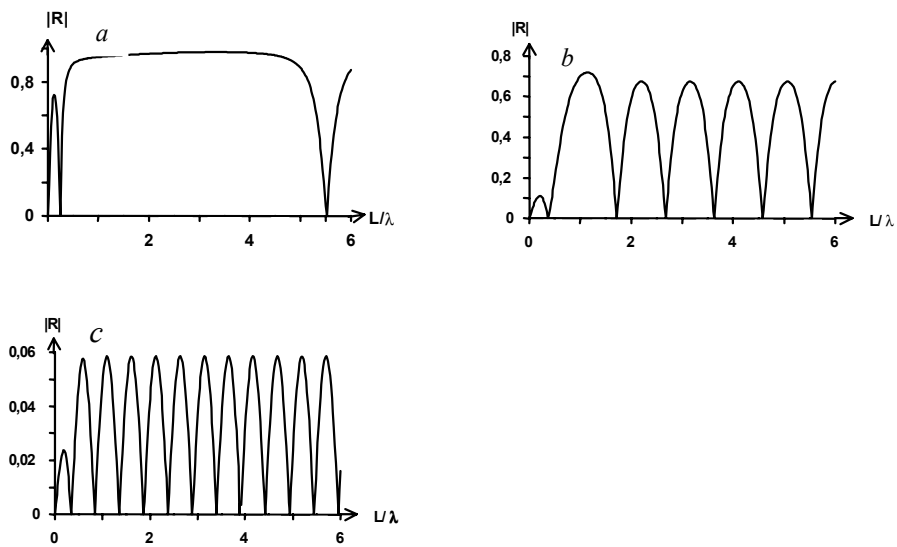


Figure2.

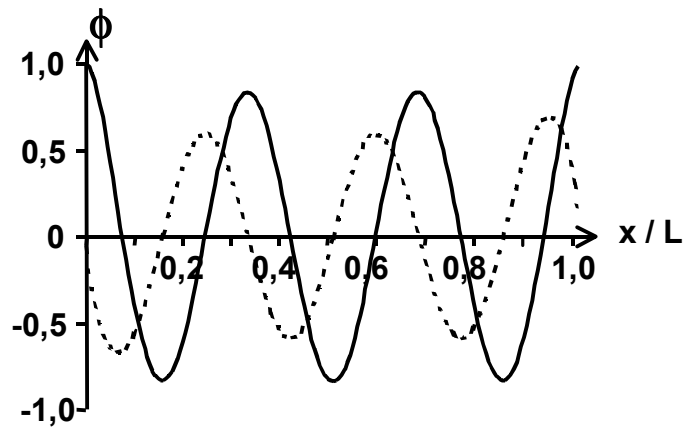


Figure3.

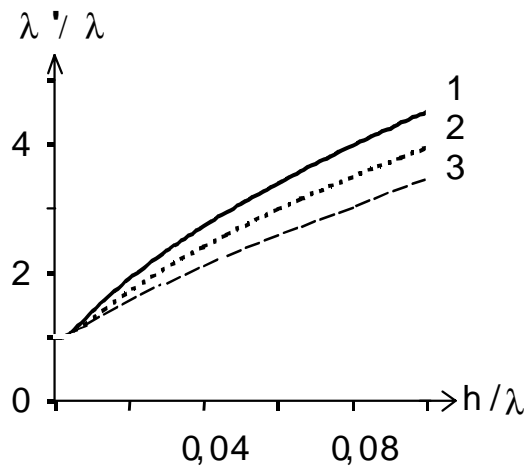


Figure 4.

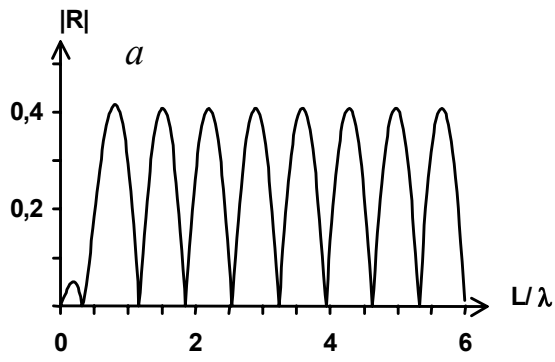


Figure5

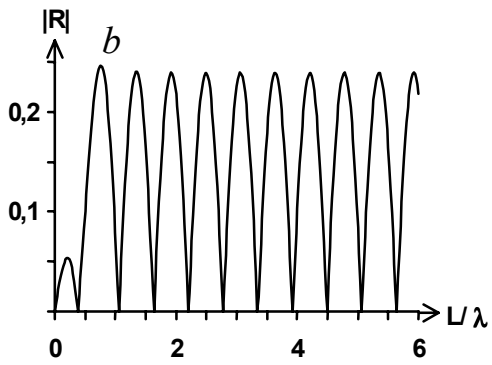


Figure 6.

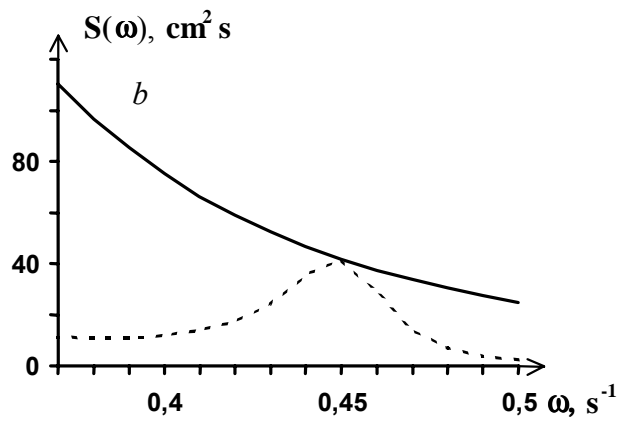
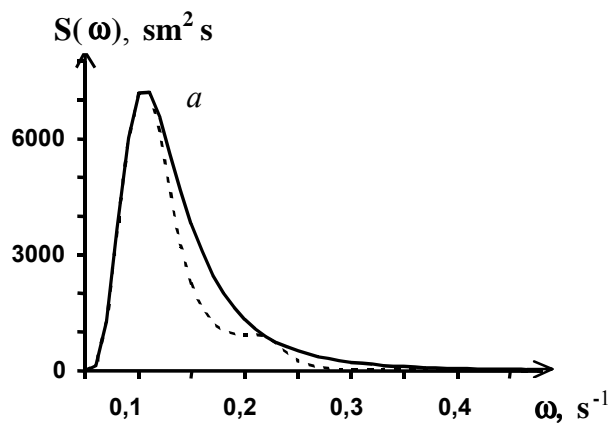


Figure 7.

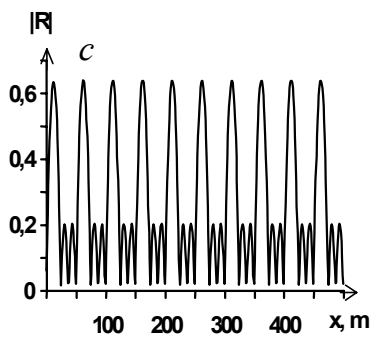
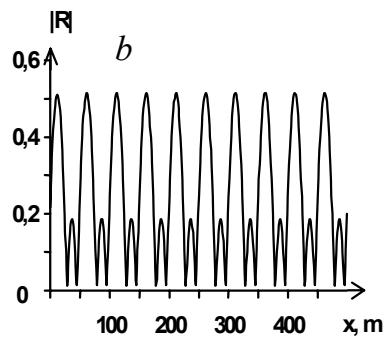
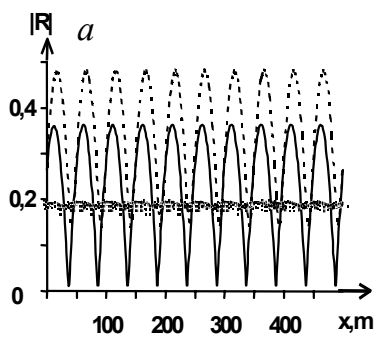


Figure 7 (a)

Captions

Figure 1. Statement of a problem

Figure 2. Proportion between the reflection coefficient $|R|$ and ice floe length L for ice thickness $h=1\text{m}$ and wave lengths $\lambda=10\text{ m}, 50\text{ m}, 200\text{ m}$ (Figs. *a, b, c* accordingly)

Figure 3. Profile of speed potential ϕ under ice floe from dimensionless coordinate x/L ($L = 366\text{ m}$). Wave length λ is equal to 100 m , ice thickness $h=1\text{ m}$. Continuous line is the real part, dotted line is imaginary part.

Figure 4. Proportion between wave length λ_r/λ under ice cover and ice thickness h/λ for wave length on open water $\lambda=50\text{ m}; 100\text{ m}; 200\text{ m}$ (curves 1–3)

Figure 5. Proportion between reflection coefficient $|R|$ and ice floe length L with wave length $\lambda=10\text{ m}$, ice thickness $h=1\text{ m}$; accounting the ice extension, the internal ice stress is $P=-10^6\text{ N/m}^2$ (*a*); accounting ice pressure, the internal ice stress is $P=10^6\text{ N/m}^2$ (*b*)

Figure 6. Spectrum of Pirson-Moskovits before and after (dotted line) waves travelling (*a*) under ice floe $L=110\text{ m}$, $h=1\text{ m}$. More detailed high-frequency range of spectrum is presented on Figure 6 (*b*).

Figure 7. Proportion between reflection coefficient $|R|$ and distance between 2 (*a*), 3 (*b*) and 4 (*c*) ice floes for wave length $\lambda=100\text{ m}$ and ice thickness $h=1\text{ m}$.

Figure 7 (a). Continuous line - two ice floes with 100 m length; dotted line - ice floes of 100 m and 150 m length; points - ice floes of 100 m and 175 m length.